Rydberg Complexes of Methyl Chloride Characterized by (2+1) and (3+1) Resonance-Enhanced Multiphoton Ionization

Michael G. Szarka,[†] David S. Green,[‡] David T. Cramb, and Stephen C. Wallace*

Department of Chemistry, University of Toronto, Toronto, Ontario, Canada M5S 1A1

Received: July 31, 1996; In Final Form: December 9, 1996[⊗]

The two- and three-photon resonant spectra of CH_3Cl have been recorded in the region of the lower Rydberg states. Assignments are made for numerous electronic and vibrational bands related to the first two members of the s, p, and d Rydberg series in CH_3Cl, extending or revising the assignments of previous workers. Comparisons of two- and three-photon spectra and polarization effects show strong contrast and reveal the varying degrees of atomic behavior in the six electronic states studied. The orbital angular momentum quantum number of the Rydberg state is shown to have a greater influence on the degree of penetration and consequent deviation from hydrogen-like orbital character than the magnitude of the principal quantum number.

Introduction

The electronic spectrum of methyl chloride has remained more poorly characterized than those of other hydrogen and methyl halides, due to greater spectral diffuseness and complicated spin−orbit coupling effects. This work presents an analysis of new multiphoton spectra of the CH_3Cl Rydberg states. The unique capabilities of multiphoton spectroscopy permit spectroscopic analysis that would be impossible to perform with conventional spectroscopic methods.

The classic analyses of the spectra of the hydrogen halides,[1−4] the methyl halides,[3−5] and the diatomic halogen molecules[6−9] constitute a series of studies by R. S. Mulliken, in which he interpreted hydrogen and methyl halide emission spectra measured by Price[10] and earlier workers.[11,12]

Felps et al.[13] studied the 4s Rydberg states of CH_3I, CH_3Br, and CH_3Cl, but were unable to determine unique assignments of the electronic origins in the case of CH_3Cl, due to the diffuseness of one-photon transitions to these states in CH_3Cl. The non-s Rydbergs in methyl iodide have been studied by both absorption spectroscopy[14] and multiphoton methods,[15,16] but methyl chloride has only been the object of single-photon absorption spectra[14,17−19] that assign the various series.

Russell and co-workers recorded and analyzed the CH_3Cl spectrum, first in the context of the mono- and polychloromethanes[17] and then in a survey of simple chloroalkanes.[18] McGlynn and co-workers[14] studied Rydberg series of CH_3X molecules, X = Cl, Br, or I, using the approach of Robin,[20] whereby Rydberg series are assigned through correlations of term values among a series of chemically similar molecules. Truch et al.[19] measured the absorption spectrum of the higher electronic transitions of CH_3Cl and assigned 60 observed peaks as Rydberg origins and vibrational progressions built on them.

The essential features of the methyl chloride spectrum, with the exception of a low-lying $\sigma^* \leftarrow \sigma$ valence transition, are attributed to electron promotion from the highest nonbonding $3p\pi$ orbital of the chlorine atom into higher atom-like or Rydberg molecular orbitals. The lowest Rydberg transition in CH_3Cl, for example, is assigned as the transition from a $...(3p\pi^4)$ configuration into a $...(3p\pi^3)4s$ configuration, that is, promotion from $3p\pi$ to the 4s nonbonding chlorine atomic orbital.[3−5]

The spectra of CH_3Cl reported in this study extend from about 60 000 to 83 000 cm^{-1}, within which six electronic states are identified. The results of the study probe the question of which Rydberg orbitals are most nearly "atomic" and which have a nonhydrogenic nature imparted by the molecular frame. Is the electronic structure most simply and effectively described as that of a distorted chlorine atom, a pseudo-diatomic analog of HCl, or is consideration of the C_{3v} symmetry of the molecule essential in interpreting its spectrum? The answer to these questions will be seen to vary significantly for the six Rydberg states studied in this work.

Experimental Section

Mass-resolved REMPI spectra were recorded using a time-of-flight mass spectrometer whose design has been reported previously.[21] Briefly, ions were generated in an extraction field between a plate at +1500 V and a grid held at −1500 V, separated by about 4 cm. A metal collimated hole structure (Brunswick Corp.) separated the ionization region from an electrostatic Einzel lens and a 1.3 m field-free drift region. A Galileo Electro-Optics Corp. chevron-type dual microchannel plate electron multiplier was used to detect the single-shot mass spectrum. This apparatus is capable of unit mass resolution at 400 amu. Ion signals at selected flight times were processed by individual gated integrators and stored by computer for further analysis.

CH_3Cl (Matheson) was rated as 99.5% and was used without further purification. Dilutions to 10% by pressure of CH_3Cl in He were prepared using UHP grade He from Canox. Molecular expansions were produced by a Newport Research Corp. pulsed valve and were directed through an inch long 500 μm capillary into the extraction region of the mass spectrometer. Valve pulse durations were 170−300 μs, and stagnation pressures used were typically 25 psi absolute. The expansions were probed in a region where rotational temperatures were estimated to be between 50 and 100 K.

The laser excitation source was a Lumonics Hyperdye 300 laser pumped at 308 nm by a Lumonics EX-700 excimer laser, or a Quanta-Ray PDL-1 dye laser pumped at 532 nm by a Quanta-Ray GCR-3 Nd:YAG laser. For production of wavelengths below 340 nm, the dye laser output was frequency doubled in β-$BaBO_3$ or KDP providing between 2 and 6 mJ of ultraviolet light. Circularly polarized light was obtained through the use of a Babinet-Soleil compensator (Karl Lambrecht Corp.).

[†] Present address: Ontario Laser and Lightwave Research Centre, Rm 331, 60 St. George St., Toronto, Ontario M5S 1A7, Canada.

[‡] Present address: National Institute of Standards and Technology, Building 221, Room A-303, Gaithersburg, MD 20899.

[⊗] Abstract published in *Advance ACS Abstracts,* February 1, 1997.

S1089-5639(96)02334-1 CCC: $14.00

The light was focused into the ionization region by a 40 cm lens in the (2+1) MPI experiments and a 30 cm lens in the (3+1) and (3+2) MPI experiments.

Spectra reported here were all accumulated by observing the *m*/*e* 15 (CH_3^+) ion signal as a function of wavelength, since it was by far the strongest mass spectral signal in all multiphoton ionization experiments, and in those cases where signals from heavier ions were strong enough to record a spectrum, no significant differences in the spectra were observed. All spectra were wavelength calibrated by simultaneous measurement of optogalvanic spectra of neon and comparison with standard tables of atomic spectral line positions.[22,23] The spectral resolution obtainable with this apparatus is better than 0.3 cm^{-1}, significantly narrower than the spectral features reported here.

All reported band positions are given to the nearest five wavenumbers and correspond to maxima in the unresolved rotational envelopes of each vibrational band, which will in general be different from the true band origins. The half-widths of the rotational envelopes are generally on the order of 100 cm^{-1} or more, and no attempt was made to model the underlying structure.

Most of the spectra shown are the result of concatenation of a number of spectral scans. It was not feasible to accurately stabilize laser intensity due to variation in laser dye gains, dielectric mirror reflection bandwidths, beam quality, frequency-doubling efficiencies, and so on. Although attempts were made to normalize adjacent spectra through intensities of overlapping bands where possible, there are evident discontinuities in some of the baseline levels and significant uncertainties in the relative intensities across scans.

Angular Momentum Coupling and Selection Rules in Rydberg States of CH_3Cl

(a) Coupling in $(\pi^3)\sigma$ Configuration Rydberg States. Interpretation of the methyl halide Rydberg spectra requires consideration of the detailed interaction of the orbital and spin angular momenta of the ion core and the Rydberg electron. The configuration of s Rydbergs in the diatomic halogen molecules and the hydrogen halides is $...(\pi^3)\sigma$, which results in $^1\Pi$ and $^3\Pi_{2,1,0}$ states in Russel−Saunders or (Λ,S) coupling. For larger spin−orbit coupling better described as (ω,ω) or (Ω_c,ω) coupling, the resulting states are labeled as $\Omega = 0$, 1, 1, and 2.[6,24] For these latter cases of significant spin−orbit interaction, the proper state symmetries are obtained by combining the spin function with the orbital function.[25] The symmetries of the spin functions for the configuration under question are $E_{1/2}$ and $E_{3/2}$ for the core and $E_{1/2}$ for the outer σ (Rydberg) electron. These correspond to species of the double or extended point group $C^*_{\infty v}$, which must be used in the case of net half-integral electronic spin.[26] Resolution of the direct product $E_{1/2}\otimes E_{1/2}$ in $C^*_{\infty v}$ results in terms Σ^+, Σ^-, and Π; for $E_{1/2}\otimes E_{3/2}$ one obtains Π and Δ.[25] The level spacings expected for the various degrees of spin−orbit coupling and the appropriate state symmetry labels are illustrated in Figure 1. The left-hand side of the figure corresponds to minimum spin−orbit coupling, while the extreme right-hand side shows maximum spin−orbit coupling, that is, the pure spin−orbit (S-O) splitting of the ionic ground state.

For the C_{3v} point group, one changes Σ^+, Σ^-, and Π to A_1, A_2, and E labels respectively. The diatomic Δ level in this lower symmetry mixes with the Π state, giving two states labeled as E (with $\Omega = 1$ or 2).[27]

The intervals between the $^1\Pi$, $^3\Pi_1$, and $^3\Pi_{0+}$ levels for intermediate S-O coupling have been given by Mulliken[8] as

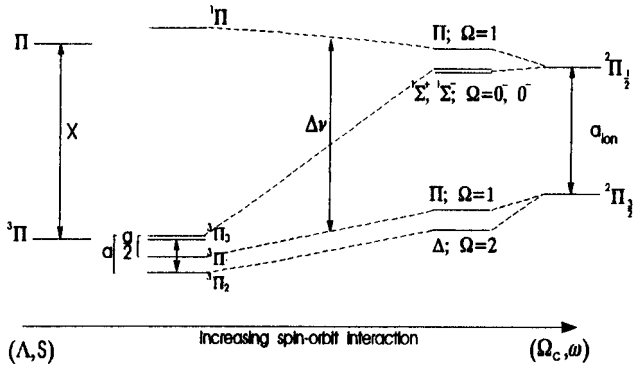

Figure 1. Correlations and energy levels for the transition between (Λ,S) and (Ω_c,ω) coupling schemes. Symbols are defined in the text.

$$E(^1\Pi) - E(^3\Pi_1) = X(1 + 1/P^2)^{1/2} \equiv \Delta\nu \quad (1)$$

$$E(^1\Pi) - E(^3\Pi_{0+}) = \Delta\nu/2 + a(\mu P - 1)/2 \quad (2)$$

$$E(^3\Pi_{0+}) - E(^3\Pi_1) = \Delta\nu/2 - a(\mu P - 1)/2 \quad (3)$$

where X is the singlet−triplet separation, a is the spin−orbit coupling coefficient for a single π electron (which would be the same as the doublet splitting in the ion), and $P \equiv X/\mu a$, where μ is a number slightly less than 1, which should approach 1 if X approaches 0.[8] The splitting between the levels gives a quantification of the transition from (Λ,S) to (Ω_c,ω) coupling, by virtue of the relative magnitudes of X and a.

For strict (Λ,S) coupling, the single-photon selection rules for transitions from the ground ($^1\Sigma^+$) state allow transitions only to $^1\Pi$ and not to any of the $^3\Pi$ components. As (Ω_c,ω) coupling is approached, the $\Omega = 1$ ($^1\Pi$ and $^3\Pi_1$) states begin to mix, with $^3\Pi_1$ stealing intensity from $^1\Pi$.[8] Transitions also become allowed to the 0^+ (Σ^+) level derived from $^3\Pi_0$, through a mechanism related to Hund's case (c) effects.[7] Single-photon transitions to the $^3\Pi_2$ or Δ and the 0^- (Σ^-) component of the $^3\Pi_0$ state remain strictly forbidden under $C_{\infty v}$. In two- or three-photon excitation, transitions to diatomic Δ states become allowed[28] (see Table 1). Transitions to Σ^- remain forbidden in any excitation scheme involving absorption of one or more photons of identical wavelength by a linear molecule. However, under C_{3v} symmetry, transitions to the corresponding A_2 bands become allowed by three-photon absorption (Table 2). The method of determination of the multiphoton selection rules is outlined in ref 28 and references quoted therein.

(b) Coupling in $(\pi^3)\pi$ Configuration Rydberg States. In the Russell−Saunders limit the symmetries are determined by the product E⊗E, giving rise to states $^3\Sigma^+$, $^3\Sigma^-$, $^3\Delta$, $^1\Sigma^+$, $^1\Sigma^-$, and $^1\Delta$. For the case of large S-O interaction, the symmetries are determined by the products of $E_{1/2}$ or $E_{3/2}$ spin functions for both the Rydberg electron and the core, giving 10 states: one $\Omega = 3$ (Φ) state, two $\Omega = 2$ (Δ) states, three $\Omega = 1$ (Π) states, two $\Omega = 0^+$ (Σ^+) states, and two $\Omega = 0^-$ (Σ^-) states.[25,28]

For small spin−orbit interaction, only transitions to the $\Omega = 0^+$ state derived from the diatomic $^1\Sigma^+$ state would be allowed. As S-O coupling increases, transitions to both of the $\Omega = 0^+$ states will become allowed as the $^1\Sigma^+$ and the $^3\Sigma^-$ states they are derived from become mixed,[8] and in the strong S-O coupling case, transitions from the ground state to the $\Omega = 1$ states will become allowed by the $\Delta\Omega = 0, \pm 1$ selection rule.

(c) Coupling in $(\pi^3)\delta$ Configuration Rydberg States. In C_{3v} symmetry, there is no basis for distinguishing the $(\pi^3)\delta$ case from $(\pi^3)\pi$, since on lowering the symmetry from $C_{\infty v}$, both π and δ correspond to species e. For diatomics, (Λ,S) coupling will result in the appearance of $^1\Pi$, $^1\Phi$, $^3\Pi$, and $^3\Phi$ states, while

TABLE 1: Allowed Transitions and Multiphoton Selection Rules in $C_{\infty v}$ for Various Combinations of Two- and Three-Photon Absorption and Incident Light Polarization[a]

transition	rank	$2h\nu$ linear	$2h\nu$ circular	$3h\nu$ linear	$3h\nu$ circular
$\Sigma^+ \leftarrow \Sigma^+$	0	$\Delta J = 0$			
	1			$\Delta J = 0, \pm 1$	
	2	$\Delta J = 0, \pm 1, \pm 2$	$\Delta J = 0, \pm 1, \pm 2$		
	3			$\Delta J = 0, \pm 1, \pm 2, \pm 3$	$\Delta J = 0, \pm 1, \pm 2, \pm 3$
$\Pi \leftarrow \Sigma^+$	1			$\Delta J = 0, \pm 1$	
	2	$\Delta J = 0, \pm 1, \pm 2$	$\Delta J = 0, \pm 1, \pm 2$		
	3			$\Delta J = 0, \pm 1, \pm 2, \pm 3$	$\Delta J = 0, \pm 1, \pm 2, \pm 3$
$\Delta \leftarrow \Sigma^+$	2	$\Delta J = 0, \pm 1, \pm 2$	$\Delta J = 0, \pm 1, \pm 2$		
	3			$\Delta J = 0, \pm 1, \pm 2, \pm 3$	$\Delta J = 0, \pm 1, \pm 2, \pm 3$
$\Phi \leftarrow \Sigma^+$	3			$\Delta J = 0, \pm 1, \pm 2, \pm 3$	$\Delta J = 0, \pm 1, \pm 2, \pm 3$

[a] The ΔK selection rules are intrinsic to the state symmetry labels, and so are omitted from the table. Transitions $\Sigma^- \leftarrow \Sigma^+$ are disallowed for any rank, and so are omitted from the table. Circularly polarized light eliminates all but the highest ranked tensor contribution to each transition. However, the intensity due to that remaining rank will increase by a factor of 3/2 for two-photon absorption and 5/2 for three-photon absorption. Additional information can be obtained from ref 28 and references therein.

TABLE 2: Allowed Transitions and Multiphoton Selection Rules in C_{3v}[a]

transition	rank	$2h\nu$ linear	$2h\nu$ circular	$3h\nu$ linear	$3h\nu$ circular
$A_1 \leftarrow A_1$	0	$\Delta K = 0$ $\Delta J = 0$			
	1			$\Delta K = 0$ $\Delta J = 0, \pm 1$	
	2	$\Delta K = 0$ $\Delta J = 0, \pm 1, \pm 2$	$\Delta K = 0$ $\Delta J = 0, \pm 1, \pm 2$		
	3			$\Delta K = 0, \pm 3$ $\Delta J = 0, \pm 1, \pm 2, \pm 3$	$\Delta K = 0, \pm 3$ $\Delta J = 0, \pm 1, \pm 2, \pm 3$
$A_2 \leftarrow A_1$	3			$\Delta K = \pm 3$ $\Delta J = 0, \pm 1, \pm 2, \pm 3$	$\Delta K = \pm 3$ $\Delta J = 0, \pm 1, \pm 2, \pm 3$
$E \leftarrow A_1$	1			$\Delta K = \pm 1$ $\Delta J = 0, \pm 1$	
	2	$\Delta K = \pm 1, \pm 2$ $\Delta J = 0, \pm 1, \pm 2$	$\Delta K = \pm 1, \pm 2$ $\Delta J = 0, \pm 1, \pm 2$		
	3			$\Delta K = \pm 1, \pm 2, \pm 3$ $\Delta J = 0, \pm 1, \pm 2, \pm 3$	$\Delta K = \pm 1, \pm 2, \pm 3$ $\Delta J = 0, \pm 1, \pm 2, \pm 3$

[a] The same polarization/intensity rules apply as discussed in the caption to Table 1.

for large spin−orbit coupling one obtains states $\Pi(\Omega{=}1)$, $\Delta(\Omega{=}2)$, $\Delta(\Omega{=}2)$, $\Phi(\Omega{=}3)$, $\Sigma^+(\Omega{=}0^+)$, $\Sigma^-(\Omega{=}0^-)$, $\Phi(\Omega{=}3)$, $\Pi(\Omega{=}1)$, and $\Gamma(\Omega{=}4)$. In this case the $(\pi^3)\delta$ configuration is closely analogous to $(\pi^3)\sigma$, since the $^1\Pi$ and $^3\Pi$ (Λ,S) states give rise to Δ, Π, Π, Σ^+, and Σ^- (Ω_c,ω) states in exactly the same way. The existence of unobserved states derived from a $(\pi^3)\delta$ configuration in the hydrogen halides has been the subject of much discussion.[1−4,6,21,25]

Rydberg States of CH_3Cl: Results and Discussion

(a) Ionization Dynamics. CH_3^+ was the most abundant ionic species observed for all of the (2+1) and (3+1) spectra recorded in this study. The heaviest ion observed with significant intensity was CH_2Cl^+, corresponding to the ejection of an H atom upon ionization. At very short wavelengths (beneath 219 nm when the two-photon energy exceeds the 90 526 cm^{-1} ionization potential)[29] the true molecular ion (CH_3Cl^+) was produced with great efficiency. This dramatic change in the mass spectrum suggests that a new mechanism for ion formation begins at this point.

Consider ionization processes for two possible cases with only slightly different photon energies: (1) (2+1) REMPI through a Rydberg state close to but below the first IP at 90 526 cm^{-1}; and (2) direct two-photon absorption to a level just above the IP.

For case 1, the three-photon energy absorbed by the molecule would total about 16.8 eV. This would place the nascent ion in the energy region of the third photoelectron band of CH_3Cl, the $\tilde{B}$ state of CH_3Cl^+. Eland et al.[32] have determined that the $\tilde{A}$ state of CH_3Cl^+ is completely predissociated to CH_3^+ and Cl, while the $\tilde{B}$ state undergoes 80% conversion from $\tilde{B}$ to $\tilde{A}$. The remaining 20% dissociate directly to CH_2Cl^+. So in the case of excitation to this region, and ignoring dissociation of neutral CH_3Cl in the two-photon resonant Rydberg states, 80% of ions formed are predicted to dissociate to CH_3^+, while 20% will lose a hydrogen atom to form CH_2Cl^+, resulting in a CH_3^+/CH_2Cl^+ ion ratio of about 4:1 for excitation of the CH_3Cl $\tilde{B}$ state.

At 250 nm the measured ratio of mass 15 (CH_3^+) to mass 49 (principally due to $CH_2{}^{35}Cl^+$) was about 10:1. The total three-photon energy would amount to 14.9 eV. In this energy region, the $\tilde{A}$ and $\tilde{B}$ state photoelectron bands of CH_3Cl^+ are overlapped. Direct and simultaneous excitation of both the $\tilde{A}$ and $\tilde{B}$ states will thus be occurring, and so the resulting CH_3^+/CH_2Cl^+ ratio is predicted to be larger than for pure $\tilde{B}$ state excitation, as is observed.

Consider now the case of direct two-photon excitation to just above the CH_3Cl ionization potential. Two-photon absorption would necessarily be nonresonant since there are no accessible states at the single-photon energy of 45 000 cm^{-1} (the CH_3Cl $\tilde{A}$ state absorption begins at around 50 000 cm^{-1}). Above the first IP autoionizing states based on Rydberg series converging on excited ion states would be expected to dominate the spectrum. The dominance of undissociated CH_3Cl^+ molecular ion signal observed in the mass spectrum above the IP indicates that these levels ionize without molecular dissociation. In this case, ions formed would necessarily be in the CH_3Cl^+ ground state. The photoelectron spectrum of CH_3Cl clearly shows that the spectrum of $\tilde{X}$ CH_3Cl^+ is much sharper than the higher ionic states and is presumably nondissociative.[27]

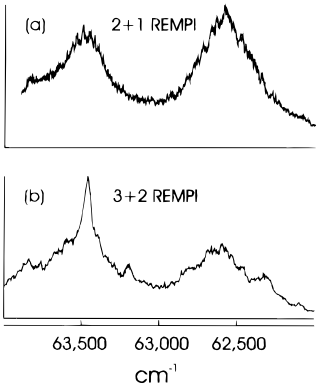

Figure 2. (a) (2+1) REMPI spectrum of 4s origin bands of CH_3Cl; (b) (3+2) REMPI spectrum of 4s origin bands of CH_3Cl.

These results are consistent with our interpretation that the mass spectral fragment patterns observed in this study are adequately explained in terms of excess energy above the IP provided by the terminal photon, and not by processes occurring in resonant states below the IP.

(b) The 4s Rydberg State of CH_3Cl. Previous absorption studies[13,14] show a very broad spectral envelope extending from about 62 000 (1600 Å) to 67 000 cm^{-1} (1500 Å) with several broad peaks superimposed. The two-photon spectrum recorded in this study is dominated by two strong and very broad peaks at 62 600 and 63 500 cm^{-1} (Figure 2), with a third broad, weaker peak centered near 65 000 cm^{-1} (not shown). The three-photon spectrum shows a more complex structure over the same wavelength range, but the same two intense peaks are the most prominent features (Figure 2).

Rabalais et al.[31] have pointed out that for molecules containing third-row atoms diminished core shielding results in quantum defects (δ) of 2.0, 1.5, and 0.4 for s-, p-, and d-type Rydberg molecular orbitals, respectively. The energies of the two most intense three-photon bands observed here at 62 590 and 63 470 cm^{-1} and the first two CH_3Cl ionization potentials at 90 526 and 91 172 cm^{-1} (separated due to the $^2\Pi$ ionic core spin−orbit splitting)[29] can be similarly inserted into the Rydberg formula.[24,31] This calculation gives an effective quantum number for this state of 2.0, consistent with the original assignment[2] of these bands as due to the 4s Rydberg state of CH_3Cl.

The most detailed studies of this region were low-pressure VUV spectra of CH_3Cl and CD_3Cl spectra taken by Felps et al.[13] These authors proposed an alternative to Mulliken's assignment[2] of the two major bands as the $^1\Pi$ and $^3\Pi_1$ components of the CH_3Cl 4s Rydberg (cf. Figure 1). However, the appearance of the band system seen in the (3+2) spectrum, in particular the weaker bands at 63 200 and 62 325 cm^{-1}, which were not seen in the Felps spectra, suggests assignments of these weaker bands as the $^3\Pi_0$ and $^3\Pi_2$ bands and the more intense bands as $^1\Pi$ and $^3\Pi_1$. Support for the identification of the 63 200 cm^{-1} band as due to the $^3\Pi_{0^+,0^-}$ states comes from the results of the polarization studies. The three-photon spectrum of this band system using circularly polarized light resulted in the extinction of all bands in the spectrum except the 63 200 cm^{-1} band. Since the $^3\Pi_{0^+,0^-}$ band will have A_1/A_2 symmetry while the other three components will all have E-type symmetry, as discussed earlier, the selection rules will be different for the bands of both types (see Table 2). These rules are discussed in more detail in the following sections.

Using eq 1 with the measured value for $\Delta\nu$ (880 cm^{-1}), the ion core splitting for a (627 cm^{-1})[32], and assuming $\mu \approx 1$, we can calculate the "ideal" singlet−triplet separation X as equal to about 619 cm^{-1}. The similar magnitudes of a and X demonstrate that this state is almost perfectly intermediate between (Λ,S) coupling and (Ω_c,ω) coupling, in accordance with Mulliken's interpretation.[4]

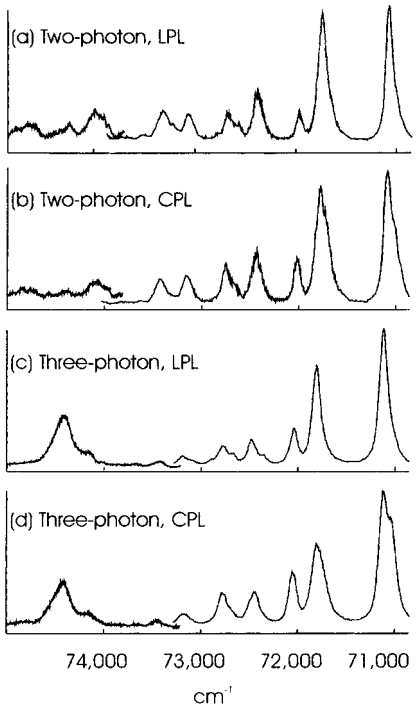

Figure 3. Two- and three-photon spectra of the 4p Rydberg region of CH_3Cl; (a) 2$h\nu$, linear polarization (LPL); (b) 2$h\nu$ circular polarization (CPL); (c) 3$h\nu$ LPL; (d) 3$h\nu$ CPL. Spectra are normalized with respect to the most intense peak in each spectrum. Baseline discontinuities result from concentration of spectra taken with different dyes. Relative intensities are subject to fluctuations over the length of each spectrum, but should be qualitatively valid for purposes of comparison. Shifts of band maxima result from changes in rotational selection rules under different excitation conditions.

(c) The CH_3Cl 4p Rydberg State: (70 000−73 000 cm^{-1}). The region above 70 000 cm^{-1} shows a sharpening of the spectral features, giving the appearance of more nearly atom-like or Rydberg character than observed in the case of the 4s state. The two- and three-photon REMPI spectra recorded in this region are shown in Figures 3 and 4. These bands have been assigned by Mulliken[4] as resulting from excitation to a 4pπ (4pe) Rydberg orbital. Solution of the Rydberg equation for the two strongest bands in this region at 71 105 and 71 775 cm^{-1} gives effective quantum numbers n^* of 2.37 and 2.38. These values suggest quantum defects of about 1.6, consistent with an assignment of these bands as origins of the 4p Rydberg state,[31] and compare well with the quantum defects for 4p Rydbergs[21] in HCl of about 1.7.

The lower origin should be the 0^+ level originating from $^1\Sigma^+$, while the upper band will be a 0^+ state derived from $^3\Sigma^-$. In the case of small spin−orbit coupling, transitions to the upper (triplet) band would not be allowed. However, as S-O coupling increases, the 0^+ ($^3\Sigma^-$) band gains intensity by mixing with the lower 0^+ ($^1\Sigma^+$) band. This interpretation is consistent with the lower intensity observed for the 71 775 cm^{-1} band. In the case of pure (Ω,ω_c) coupling, transitions to states with $\Omega = 1$ should be allowed in the absorption spectrum, but have not been reported for any of the methyl halides.

The 665 cm^{-1} separation of the two origin bands is close to the ionic ground state S-O splitting[32] of 627 cm^{-1}, and thus the S-O coupling description is more nearly (Ω_c,ω) than (Λ,S). Actually, for the case of pπ Rydberg orbitals, the splitting of

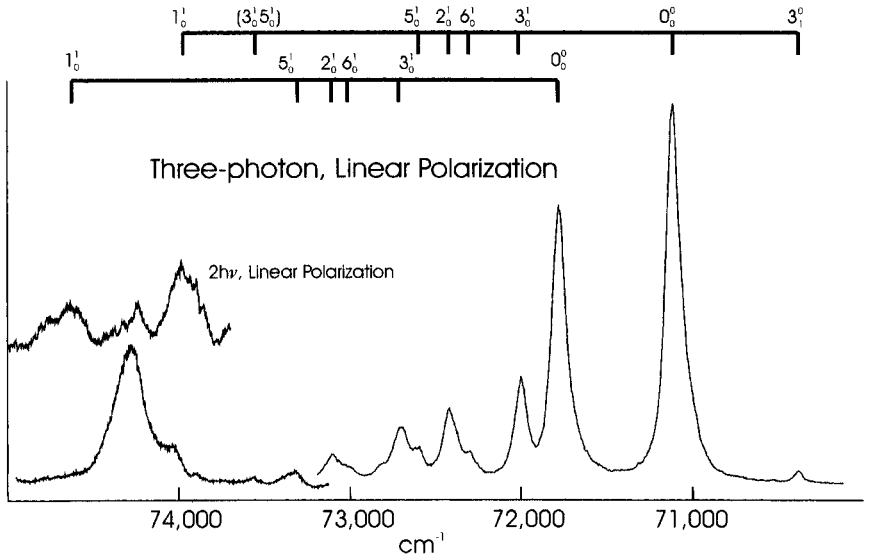

Figure 4. Spectral assignments for the 4p Rydberg region of CH_3Cl. The three-photon (LPL) spectrum is shown, with a segment of the two-photon spectrum inserted as an aid to viewing bands that were weaker in three-photon absorption. Baseline discontinuity is a result of laser dye changes and other variables as discussed in the Experimental Section. The assignment of the intense band above 74 000 cm^{-1} as the 3d state is discussed in the text.

the levels in pure (Ω_c,ω) coupling should be slightly smaller than the ion ground state doublet splitting (lowered by the magnitude of the spin−orbit coupling for the pπ Rydberg electron with itself).[4] The measured splitting suggests the presence of minor contributions from exchange energy in 4p CH_3Cl, although less than observed in the 4s state.

Truch et al.[19] assigned several weaker spectral features as vibrational bands built on the 4p origins. The multiphoton spectra reported here suggest altered assignments of the vibrational bands (see Table 3 and Figure 3). Table 4 contains the symmetries and designations of the fundamental vibrations of CH_3Cl and compares the vibrational frequencies determined here for the 4p Rydberg states with those previously determined for the ground state[33] and the ion.[29,32] The assigned vibrational frequencies are in general very close to those of the CH_3Cl ground state, with the single exception of a moderate increase in the C−Cl stretching frequency. This supports the prediction that the excited electron is essentially nonbonding in character.[4]

An important point to note from Table 3 is that transitions are assignable to all of the CH_3Cl fundamentals. Since ν_4, ν_5, and ν_6 are degenerate vibrations of species E, transitions with Δv (E) odd are forbidden in single-photon absorption in the absence of vibronic interaction or a change in molecular shape.[25] Since two-photon absorption can be characterized as a sequence of single-photon absorption events through a virtual state,[34] the vibrational selection rule must hold for each individual absorption step, so that the odd members of progressions of degenerate vibrations should be forbidden even in a multiphoton spectrum.

If the electronic levels involved are degenerate, forbidden vibrations can become vibronically allowed due to Jahn−Teller interactions.[25] If the orbitals in question are indeed pπ Rydbergs, the two most intense origin bands are expected to be nondegenerate 0^+ (A_1) states, and so Jahn−Teller vibronic splittings will be impossible. On the other hand, if the bands were due to 4pσ, they would have degenerate symmetries $^3\Pi$ and $^1\Pi$ (^{3}E and ^{1}E). In HCl, 11 band systems arising from both 4pσ and 4pπ Rydberg orbitals have been assigned in one- and two-photon absorption.[21,35]

The discernible broadening of the 4p origin bands under CPL in Figure 3 could suggest the presence of unresolved bands such as 4pσ to the red of the main origin peaks. However, an alternative explanation, proposed by Whetten and Grant,[36] suggests that the existence of the degenerate vibrations can be rationalized with reference to the analysis of vibronic coupling in the Rydberg states of benzene. They argued that nondegenerate Rydberg states based on a degenerate ion state can display vibronic structure characteristic of a degenerate state. This explanation removes the need to alter the original assignments of these origins as due to 4pπ.

TABLE 3: Band Positions and Assignments for CH_3Cl 4p Rydberg States[a]

energy (cm^{-1})	$\Delta\nu$ (cm^{-1}) from origin [ ]	previous assignment[19]	new assignment, comments
70 370	−735 [1]		3_1^0 [1]
71 105 origin [1]		4pe′	($^2E_{3/2}$)4p
71 775 origin[2]	(670 [1])	4pe″	($^2E_{1/2}$)4p
71 995	890 [1]	6_0^1 [1]	3_0^1 [1]
72 295	1190 [1]		6_0^1 [1]
72 415	1310 [1]	2_0^1 [2]	2_0^1 [1]
72 590	1485 [1]	6_0^1 [2]	5_0^1 [1]
72 700	925 [2]		3_0^1 [2]
72 815			? weak
73 100	1325 [2]	2_0^1 [2]	2_0^1 [2], low-energy shoulder is probably 6_0^1 [2]
73 245	1470 [2]	$2_0^1 + 6_0^1$ [1]	5_0^1 [2]
73 340	2235 [1] 1565 [2]		probably $2_0^1 + 3_0^1$ [1]
73 545	2440 [1] 1770 [2]		weak, possibly $3_0^1 + 5_0^1$ [1]
73 975	2870 [1]		1_0^1 [1]
74 245	3140 [1]		4_0^1 [1]
74 275		$4pa_1$	3d; weak in 2+1, strong in 3+1
74 715	2940 [2]		1_0^1 [2]
74 945	3170 [2]		4_0^1 [2]

[a] Symmetry of the 4p origins is uncertain, possibly comprising overlapped 4pσ and 4pπ, and are therefore labeled here only by the 4p orbital designation with respect to a specific ion core.

(d) The CH_3Cl 3d Rydberg State (74 000−77 000 cm^{-1}). The main feature in REMPI spectra of this region is a band at 74 275 cm^{-1}, which is strong in three-photon absorption but weak in the two-photon spectrum (Figures 3 and 4). This peak,

TABLE 4: CH_3Cl Vibrational Frequencies (cm^{-1})

vibration	ground state[33]	ionic ground state[29,32]	4p Rydberg (average)
ν_1 (A_1) C−H stretch (symmetric)	2937		2905
ν_2 (A_1) C−H_3 umbrella	1355	1514 (?)	1320
ν_3 (A_1) C−Cl stretch	732	871	910
ν_4 (E) C-H stretch	3039		3155
ν_5 (*E*) C−H deformation	1452	1550 (?)	1480
ν_6 (E) C−H_3 rock	1017	924 or 968	1190

which is also prominent in the single-photon CH_3Cl absorption spectrum,[19] has been alternately assigned as a transition to either a 4p(a_1) state,[19] a 3d Rydberg state approaching the $^2\Pi$ ionic ground state,[14] or the lowest Rydberg state approaching the first excited state of the CH_3Cl^+ ion ($^2A_1$).[8] This band lacks a visible spin−orbit partner, which has been the source of much of the controversy in its assignment.

According to the multiphoton selection rules summarized in Table 2, the only bands observable in three-photon but forbidden for all ranks in two-photon REMPI would be those with A_2 symmetry. These bands would also be forbidden in single-photon absorption. Since the 74 275 cm^{-1} band is strong in the one-photon absorption spectrum,[19] the upper state cannot have symmetry A_2. Polarization studies of the band show only minor effects (Figure 4). The symmetry selection rules thus leave the two- and three-photon contrast apparent in Figure 4 unexplained.

The most recent assignment of this band by Truch et al.[19] was as a 4pa_1 (4pσ) Rydberg. This assignment presents no explanation for the lack of a spin−orbit partner nor for the marked contrast between the two- and three-photon intensities.

The assignment of this band as a σ Rydberg orbital combining with a $^2A_1$ (σ,π^4) excited ion core (CH_3Cl^+ $\tilde{A}$), as proposed by Raymonda et al.,[8] would imply the existence of $^3A_1$ and $^1A_1$ levels. Since both the Rydberg electron and the core would have zero orbital angular momentum, there could be no spin−orbit coupling, and as a result, transitions to the $^3A_1$ level would be forbidden. While this assignment explains the single-band spectrum, it does not account for the two- and three-photon intensity contrast.

The value for the quantum defect for this band suggests that it is not related to an excited ion state. The effective principal quantum number of this band is about 2.6 with respect to the first IP. If this state is related to the lowest IP, the next series members would be expected to occur near 82 100 cm^{-1}. A three-photon absorption peak at 82 285 cm^{-1} with weaker satellites at 81 755 and 83 015 cm^{-1} can be seen in the three-photon CH_3Cl spectrum (Figure 5). These features are absent/weak in two-photon absorption, as is the 74 275 cm^{-1} peak. These are the only other bands observed in this study that exhibit this behavior, suggesting that these bands are part of the same series and that the 74 275 cm^{-1} band is related to the lowest IP and not an excited state.

Consider a possible assignment of this band as the 3d Rydberg state, as suggested by Hochmann et al.[14] The quantum defect δ is 0.4, an appropriate value for a d Rydberg in a molecule containing a third-row atom.[31] Series based on d Rydbergs have been assigned and theoretically modeled for both CH_3I and CH_3Br[14,37,38] and are thus reasonably anticipated to be present in CH_3Cl.

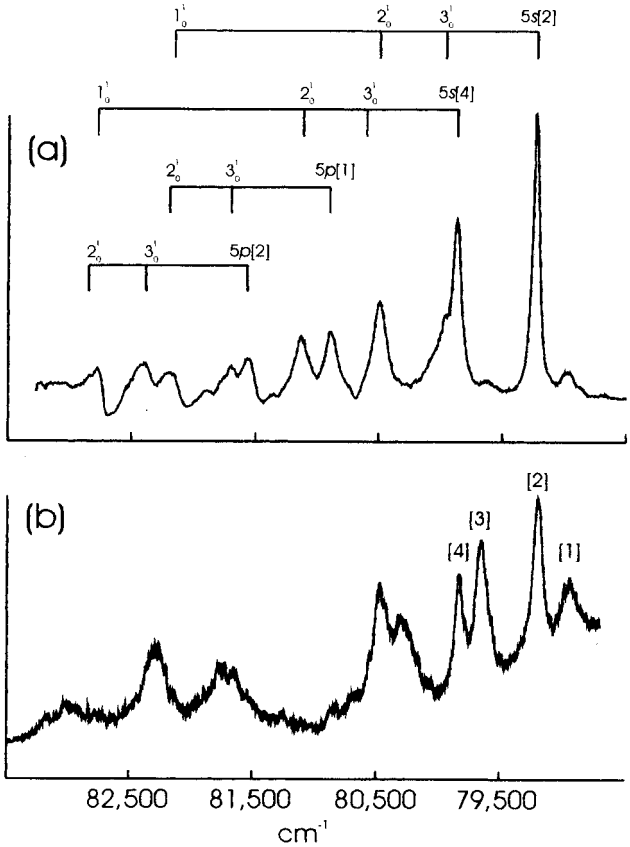

Figure 5. (a) Two-photon spectrum of CH_3Cl in the region of the 5s, 5p, and 4d Rydberg bands; (b) Three-photon spectrum. State labels [1], [2], [3], and [4] are explained in the text with reference to Figure 1.

TABLE 5: Term Values (cm^{-1}): Values for CH_3Cl Orbitals Are Based on Assignments in the Present Work

species	4s	4p	3d	4f	4d
Cl (atomic)[39]	33 000	22 100	16 900	7500	9300
CH_3Cl	28 500	19 500	16 200		8200

A comparison of the term values for atomic chlorine with those obtained for the lower orbitals in CH_3Cl is shown in Table 5. The favorable correspondence in term values[22] between the atomic Cl 3d state and the band under consideration implies a relatively nonpenetrating d orbital of highly Cl atomic character. This atomic character helps to supply an explanation for the intensity contrast of these bands in the two- and three-photon spectra.

For single-electron atomic transitions, the selection rule $\Delta l = \pm 1$ for the excited electron applies.[39] The nonbonding Cl atomic orbitals where the electron originates have been identified by Mulliken as 3p.[4] Single-photon transitions obeying the Δl selection rule would thus terminate only in s or d type orbitals (p → s, p → d, p ↛ p). Absorption of a subsequent photon by an electron excited to s or d Rydberg orbitals would promote it to either a p or f Rydberg orbital. It is impossible, therefore, for a two-photon transition to end in a d Rydberg if the atomic selection rules are to be obeyed. The polarization effects are weak and do not clearly correspond to either A_1 or E orbital symmetry, an observation which is also suggestive of atomic behavior. Such an appeal to atomic selection rules has also recently proven of value in interpreting the multiphoton spectrum of CO, where the Δl atomic selection rule has been seen to hold, to a good approximation, in the molecular spectrum.[40]

The Δl atomic selection rule seems to apply only for the case of the d orbitals. For example, Figure 4 shows clearly that the

4p Rydberg is strong in both two- and three-photon absorption. Presumably, the higher degree of molecular penetration of s and p Rydberg orbitals negates the applicability of the atomic selection rule.

Theoretical support for this interpretation of the d Rydberg structure may be found by analogy with the results of multichannel quantum defect calculations on the Rydberg structure of CH_3I,[38,41−43] which were based on comparison with similar calculations[44] on Xe. The potential seen by the electron can be written as

$$V(r) = V_C(r) + V_a(r) + V_m(R) \qquad (4)$$

where $V_C(r)$ is the dominant coulomb potential, $V_a(r)$ is an atomic potential of finite effective radius, and $V_m(r)$ is the anisotropic molecular potential. For small r the separability of the radial and angular parts of the Schrödinger equation is impaired by the presence of $V_m(r)$, and so the Rydberg electron's l is not a good quantum number. However, the results of quantum defect analysis on CH_3I suggest that for $l \geq 2$, $V_m(r)$ is not effective.[38] In other words, a d Rydberg orbital is predicted to be highly atomic in nature, supporting the unusual invocation of atomic selection rules.

The final mystery concerns the single-band structure of this state, that is, the lack of a spin−orbit partner. Lu[44] has noted in his quantum defect analysis of the Xe spectrum, on which the CH_3I calculations were based, that the LS coupling classification of the $e^- + Xe^+$ complex holds approximately, but only for $l = 2$. Thus d Rydberg electrons would produce uniquely well-defined singlet and triplet states, whereby the triplet bands would likely be too weak to be observed. The quantum defect calculations thus explain the anomalous characteristics of this band and support its assignment as the 3d Rydberg state of CH_3Cl.

(e) The 5s Rydberg State of CH_3Cl: (77 000−83 000 cm^{-1}). The (2+1) and (3+1) spectra of the 5s region of CH_3Cl are shown in Figure 5. The most intense band in two-photon absorption occurs at 79 230 cm^{-1}, for which application of the Rydberg equation gives a value of about 3.1 for n^*, consistent with the assignments of Truch et al.[19] and Hochmann et al.[14] of this band as a 5s origin. Above 80 000 cm^{-1} (1250 Å), vibrational bands built on the 5s Rydberg origins are overlapped with bands belonging to the 5p and 4d Rydberg states and are tabulated in Table 6 up to just above 83 000 cm^{-1} (1200 Å) where more severe spectral congestion sets in. The 5s vibrational band assignments are based on the vibrational frequencies of CH_3Cl and CH_3Cl^+ and those of the CH_3Cl 4p state shown in Table 4.

A tendency toward (Ω_c,ω) coupling should lead to an energy level manifold as in Figure 1 rather than a pair of well-defined $^3\Pi$ and $^1\Pi$ states as predicted by (Λ,S) coupling. It will be convenient to refer to these states in order of increasing energy as states [1] (Δ or E); [2] (Π or E); [3] (Σ^+/Σ^- or A_1/A_2); and [4] (Π or E), using diatomic symmetry labels or C_{3v} labels, respectively (Figure 5, bottom).

Bands [2] and [4] are assigned as the Π bands shown on the right side of Figure 1. They are separated by about 635 cm^{-1}, in good accord with the spin−orbit splitting of the $^2E_{1/2}$ and $^2E_{3/2}$ CH_3Cl^+ ion ground state, implying well-defined (Ω_c,ω) coupling. The peaks to lower energy of each of the stronger peaks are assigned as the $^3\Pi_2$ [1] and the $^3\Pi_{0^+,0^-}$ [3] states (cf. Figure 1).

Confirmation of these assignments comes from a consideration of the appropriate selection rules and the polarization results. The LPL and CPL three-photon spectra are shown in Figure 6, adjusted to give equal maximum intensities for the benefit of illustration. Bands [1], [2], and [4] are expected to have the same E-type symmetry and therefore the same behavior (moderate broadening of the rotational contour) under CPL (see Table 2). However, band [1] is seen to increase in intensity relative to bands [2] and [4]. This can be rationalized by recalling that state [1] correlates with a state of Δ symmetry in the $C_{\infty v}$ basis (Figure 1), while bands [2] and [4] correlate with diatomic Π states. Three-photon transitions to Δ states in $C_{\infty v}$

TABLE 6: Assignments for the 5s and 5p Rydberg States of CH_3Cl[a]

position (cm^{-1})	O (cm^{-1})	previous assignment[19]	new assignment, comments
78 970	0 (5s [1])		5s [1] ($^3E_2$)
79 230	0 (5s [2])	$5sa_1$	5s [2] ($^3E_1$)
79 685	0 (5s [3])		5s [3] ($^3E_{0^+,0^-}$)
79 865	0 (5s [4])	$5sa_1'$	5s [4] (^1E)
79 980	750 (5s [2])		5s [2] (3_0^1)
80 210	1240 (5s [1])		5s [1] 2_0^1; 3+1 only
80 505	1275 (5s [2])	$5sa_1\ 2_0^1$	5s [2] 2_0^1
80 905	0 (5p [1])		5p [1] ($^1A_1$, 0^+)
81 140	1275 (5s [4])	$5sa_1'\ 2_0^1$	5s [4] 2_0^1
81 360	1495 (5s [4])		5s [4] 5_0^1 (?)
81 570	0 (5p [2])	$5pa_1$	5p [2] ($^3A_2$, 0^+)
	665 (5p [1])		
81 700	795 (5p [1])	5pe	5p [1] 3_0^1
81 755	0 (4d [1])		4d [1] 3+1 only
81 890	2920 (5s [1])		5s [1] 1_0^1
82 190	1285 (5p [1])		5p [1] 2_0^1
82 285	0 4d [2]	5pe′	4d [2]; 3+1 only
	530 4d [1]		
82 400	830 (5p [2])	5pe 6_0^1	5p (2) 3_0^1
82 775	2910 (5s [4])	$5pa_1\ 2_0^1$	5s (4) 1_0^1
83 015	0 4d [3]	5pe 2_0^1	4d [3] or 3_0^1 4d [2]; 3+1 only
	730 4d [2]		

[a] Frequency shifts given are relative to the specified origin. (M,S) coupling designations are retained here for clarity.

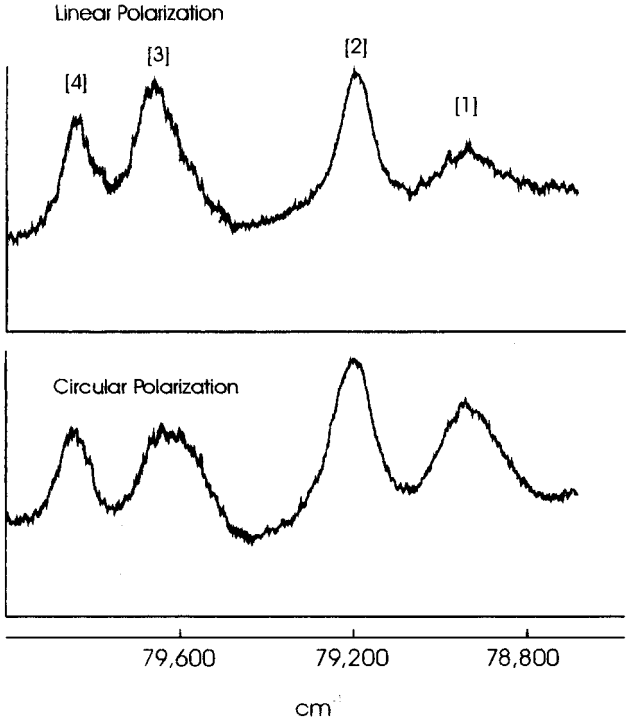

Figure 6. Polarization effects in three-photon REMPI of the CH_3Cl 5s Rydberg origins. Numbered peak designations are as described in the text with reference to Figure 1: (top) Linear polarization; (bottom) circular polarization. Spectral intensities have been normalized with respect to the most intense peak in each spectrum to better highlight the changes in band contour.

will be carried only by third rank, while transitions to Π states will have contributions from both first and third rank, where the first-rank contribution vanishes with CPL. Thus, while a Δ state should undergo a straightforward enhancement to all rotational branches with CPL, the loss of the first-rank component will cause Π states to suffer a depletion of intensity in P, Q, and R ($\Delta J = 0, \pm 1$) rotational branches relative to N, O, S, and T branches ($\Delta J = \pm 2, \pm 3$). The result is that the enhancement of band maxima for [2] and [4] is less than that of band [1].

Note that this invocation of diatomic symmetry as a basis necessarily precludes effects related to changes in the rotational top axis angular momentum Δ*K*. For a perpendicular transition in a nonlinear symmetric top molecule, rotational structure based on nonzero Δ*K* would be expected to dominate the spectral appearance. Mulliken and Teller[5] have discussed the pseudo-diatomic nature of methyl halide spectra in their description of the perpendicular $\Sigma^+ \rightarrow \Pi$ bands of the 6s Rydberg state of CH_3I, which appear to have the rotational structure characteristic of a parallel-type ($\Sigma^+ \rightarrow \Sigma^+$) transition. They noted that in a perpendicular transition in a polyatomic molecule, the angular momentum imparted results in nuclear rotation about the top axis. In a diatomic molecule, this angular momentum results in increased electronic angular momentum about the top axis. Mulliken and Teller[5] showed that in methyl iodide the three off-axis hydrogen atoms only very slightly impede the electronic motion, such that the angular momentum is not reflected in nuclear rotation, and the resulting spectrum appears like a parallel band. In effect, the rotational structure resembles that of a linear molecule where K structure cannot appear. Recently Dagata et al.[45] have modified the Mulliken−Teller interpretation to include the effects of spin uncoupling. The basic model nevertheless results in an elegant and simple explanation for the mimicry of diatomic spectral behavior seen in the methyl halides.

Band [3] should exhibit polarization behavior characteristic of a combination of A_1 and A_2. In single or two-photon absorption, $A_1 \rightarrow A_2$ transitions are strictly forbidden. In three-photon absorption, however, transitions are allowed to all symmetry types. The allowedness of $A_1 \rightarrow A_2$ transitions is particularly noteworthy since the analogous $\Sigma^+ \rightarrow \Sigma^-$ transition is forbidden under $C_{\infty v}$ by one-, two-, or three-photon absorption, so that the cylindrical symmetry-breaking of the three H atoms causes the transition to become allowed. Since transitions to A_2 are carried only by third rank, they will be expected to undergo an overall intensity enhancement with CPL. On the other hand, transitions to the A_1 component contain both first- and third-rank contributions, of which the first-rank part will disappear with CPL.

Examination of the polarization effects on band [3] (Figure 6) reveals a small decrease in intensity with CPL, but more interestingly shows an approximately 35 cm^{-1} red-shift of the band center not seen in the other three bands. Since the central rotational branches of the A_1 component should be partially diminished with CPL while the A_2 component should be enhanced, this red-shift could result from an enhancement of the A_2 component, predicted by Mulliken and Van Vleck[8,46] to be lower in energy than the A_1 component.

(f) The 4d and 5p Rydberg States (above 80 000 cm^{-1}). Based on the quantum defect for the 4p Rydberg state, the position of the lower 5p origin band is predicted by the Rydberg formula to be found at 80 900 cm^{-1}. A band of moderate intensity is observed at this position in the (2+1) REMPI spectrum (Figure 5). This band does not appear to correspond to a vibration based on either of the 5s origins (refer to Tables 4 and 6). A slightly less intense peak is located 665 cm^{-1} beyond this band, separated by precisely the same splitting as the 4p Rydberg origins. These bands are assigned as the 5p origins, which places them in different positions than reported by previous authors.[14,19]

Vibrational bands supporting the 5p origin assignments are illustrated in Figure 5, and the peak positions up to 83 500 cm^{-1} are listed in Table 6. Although only a few vibrations based on the 5p origins are assigned, the resulting vibrational frequencies are in very good accord with those assigned above for the 4p Rydberg state.

Dagata et al.[37] have observed that the p series in CH_3I is weak and disappears after the first few members. In Figure 5, the bands assigned as the 5p origins can be seen to be moderately intense in two-photon absorption, but essentially absent from the three-photon spectrum. Imposition of atomic selection rules, as discussed above for the 3d Rydberg state, would favor the appearance of p Rydbergs for even-numbered photon transitions, as appears to be the case. The lower energy 4p Rydberg transitions are strong in both (2+1) and (3+1) spectra (Figure 4), so that the higher penetration at lower *n* would seem to negate the applicability of the atomic selection rules.

Centered around 82 300 cm^{-1} is a group of three bands, whose assignment as due to the 4d Rydberg state has already been discussed. These bands are listed in Table 6 as 4d [1], [2], and [3]. Hochmann et al.[14] assigned the 4d Rydbergs for CH_3Cl as appearing at 81 666 and 82 291 cm^{-1}, in good agreement with this assignment. Specific assignments for each of the three bands are uncertain.

Conclusions

New assignments of the CH_3Cl spectrum are summarized in Tables 3 and 6. The interpretation of these results has been made within a context of the transition of the properties of the CH_3Cl states from those typical of valence states to those better described as pseudoatomic Rydberg states. The degree of Rydberg character can be considered in the following terms: the degree to which the Rydberg electron is influenced by the nature of the ionic core; the degree to which the ionic framework is influenced by the Rydberg electron; and the quantum numbers for which the ion core and the Rydberg electron truly decouple from each other's influence, such that the spectrum is more aptly described by its atomic properties.

Consider the influence of ionic core penetration on the CH_3-Cl Rydberg orbitals. For the 4s Rydberg state, there is significant penetration of the core, as evidenced by the exchange splitting and strong polarization effects. For the 5s state, the exchange effect is diminished, while the polarization behavior is intermediate between that expected for a linear versus a C_{3v} molecule, thus implying a diminished influence of molecular geometry on the spectral properties.

The 4p Rydberg orbitals show a spin−orbit splitting closer to the ionic splitting than seen for the 4s bands, while diminishing penetration up the series is evidenced by a greater conformity with the atomic selection rules by the 5p as opposed to the 4p state.

The d Rydberg orbitals are seen to be highly atomic in nature, as shown by their adherence to the atomic selection rules for multiphoton absorption and the very small polarization effects observed. On the other hand, the 3d state exhibits weak spin−orbit coupling, such that it appears as an isolated singlet band. This trend away from an (Ω_c,ω) coupling model is best considered in terms of (L,S) coupling instead of (Λ,S) coupling, as has been discussed earlier. An essentially spherically

symmetric ion core (as far as the Rydberg electron is concerned) would still produce well-defined singlet and triplet states. The Rydberg electron thus appears to probe the core to the extent of being strongly influenced by its orbital and spin angular momenta, but not by the molecular geometry. The multiple bands related to the 4d Rydberg orbital suggest a probable transition away from (L,S) coupling with the core at higher principal quantum numbers.

The influence of the Rydberg electron on the core will be manifested by changes in the vibrational frequencies. Well-defined vibrational structure was observed only for the 4p Rydberg and to a lesser extent the 5s state. Results shown in Tables 3, 4, and 6 reveal that most of the vibrational frequencies observed for the Rydberg states vary only slightly from the values for the CH_3Cl ground state. The exceptions are ν_3 and ν_6, the C−Cl stretch and the methyl rock, which relate to the stiffness of the C−Cl bond. An increase of the C−Cl stretching frequency in the ion seems clearly enough established[29,32] to suggest that this effect is intrinsic to the core and not due to the Rydberg electron. On the other hand, the diffuseness of most of the CH_3Cl bands suggests a short lifetime for the Rydberg states. Since the ground ionic state is a comparatively sharp transition[29] (implying a bound state), the Rydberg electron must have some interaction with the atomic frame.

The results of this study suggest that the overall decoupling of the CH_3Cl Rydberg orbitals from the core progresses rapidly with increasing quantum number and even more strongly in the sense $d \gg p > s$.

Acknowledgment. This research was made possible by grants funded by the Network of Centres of Excellence Programme in association with the Natural Sciences and Engineering Research Council of Canada and by the Ontario Laser and Lightwave Research Centre. An NSERC postgraduate research scholarship for M.S. is gratefully acknowledged.

References and Notes

(1) Mulliken, R. S. *Phys. Rev.* **1936**, *50*, 1017.
(2) Mulliken, R. S. *Phys. Rev.* **1937,** *51*, 310.
(3) Mulliken, R. S. *Phys. Rev.* **1935**, *47*, 413.
(4) Mulliken, R. S. *Phys. Rev*. **1942**, *61*, 277.
(5) Mulliken, R. S.; Teller, E. *Phys. Rev.* **1942**, *61*, 283.
(6) Mulliken, R. S. *Phys. Rev.* **1934**, *46*, 549.
(7) Mulliken, R. S. *J. Chem. Phys.* **1936**, *4*, 620.
(8) Mulliken, R. S. *Phys. Rev.* **1940**, *57*, 500.
(9) Mulliken, R. S. *J. Chem. Phys.* **1940**, *8*, 234.
(10) Price, W. C. *J. Chem. Phys.* **1936**, *4*, 539.
(11) (a) Heinrici, A. *Z. Phys.* **1932**, *77*, 35. (b) Heinrici, A.; Grieneisen, H. *Z. Phys. Chem. B.* **1935**, *30*, 1.
(12) Herzberg, G.; Scheibe, G. *Z. Phys. Chem. B* **1930**, *7*, 390.
(13) Felps, S.; Hochmann, P.; Brint, P.; McGlynn, S. P. *J. Mol. Spectrosc.* **1976**, *59*, 355.
(14) Hochmann, P.; Templet, P. H.; Wang, H.-t.; McGlynn, S. P. *J. Chem. Phys.* **1975**, *62*, 2588.
(15) Dobber, M. R.; Buma, W. J.; de Lange, C. A. *J. Chem. Phys.* **1993**, *99*, 836.
(16) Gedanken, A.; Robin, M. B.; Yafet, Y. *J. Chem. Phys.* **1982**, *76*, 4798.
(17) Russel, B. R.; Edwards, L. O.; Raymonda, J. W. *J. Am. Chem. Soc.* **1973**, *95*, 2129.
(18) Raymonda, J. W.; Edwards, L. O.; Russell, B. R. *J. Am. Chem. Soc.* **1974**, *96*, 1708.
(19) Truch, D. T.; Salomon, D. R.; Armstrong, D. A. *J. Mol. Spectrosc.* **1979**, *78*, 31.
(20) Robin, M. B. *Higher Excited States of Polyatomic Molecules*; Academic: New York, 1969; Vol. 1.
(21) (a) Green, D. S. Ph.D. Thesis, University of Toronto, 1990. (b) Green, D. S.; Bickel, G. A.; Wallace, S. C. *J. Mol. Spectrosc.* **1991**, *150*, 303. (c) Green, D. S.; Bickel, G. A.; Wallace, S. C. *J. Mol. Spectrosc.* **1991**, *150*, 354. (d) Green, D. S.; Bickel, G. A.; Wallace, S. C. *J. Mol. Spectrosc.* **1991**, *150*, 388.
(22) Striganov, A. R.; Sventitskii, N. S. *Tables of Spectral Lines of Neutral and Ionized Atoms*; Plenum Press: New York, 1968.
(23) Phelps, F. M., III. *Massechusetts Institute of Technology Wavelength Tables*, Vol. 2 Wavelength by Element; The MIT Press: Cambridge, MA, 1982.
(24) Herzberg, G. *Molecular Spectra and Molecular Structure*; Van Nostrand: New York, 1950; Vol. 1.
(25) Herzberg, G. *Molecular Spectra and Molecular Structure*; Van Nostrand: New York, 1966; Vol. 3.
(26) Herzberg, G. *Discuss. Faraday Soc*. **1963**, *35*, 7.
(27) Parker, D. H.; Pandolfi, R.; Stannard, P. R.; El-Sayed, M. A. *Chem. Phys*. **1980**, *45*, 27.
(28) Szarka, M. G. Ph.D. Thesis, University of Toronto, 1993.
(29) Turner, D. W.; Baker, C.; Baker, A. D.; Brundle, C. R. *Molecular Photoelectron Spectroscopy*; Wiley-Interscience: London, 1967.
(30) Eland, J. H. D; Frey, R.; Kuestler, A.; Schulte, H.; Brehm, B. *Int. J. Mass Spectrom. Ion Phys*. **1976**, *22*, 155.
(31) Rabalais, J. W.; McDonald, J. M.; Scherr, V.; McGlynn, S. P. *Chem. Rev.* **1971**, *71*, 73.
(32) Ragle, J. L.; Stenhouse, I. A.; Frost, D. C.; McDowell, C. A. *J. Chem. Phys*. **1970**, *53*, 178.
(33) (a) Shimanouchi, T. *Table of Molecular Vibrational Frequencies*; Nat. Bur. Stand. U. S., NSRDS-S: Washington DC, 1972; Vol. 1. (b) Herzberg, G. *Molecular Spectra and Molecular Structure*; Kreiger Publishing: Malabar, FL, 1991; Vol. II.
(34) Metz, F.; Howard, W. E.; Wunsch, L.; Neusser, H. J.; Schlag, E. W. *Proc. R. Soc. London A* **1978**, *363*, 381.
(35) Tilford, S. G.; Ginter, M. L. *J. Mol. Spectrosc*. **1971**, *40*, 508.
(36) Whetten, R. L.; Grant, E. R. *J. Chem. Phys*. **1984**, *80*, 5999.
(37) Dagata, J. A.; Findley, G. L.; McGlynn, S. P.; Connerade, J. P.; Baig, M. A. *Phys. Rev. A* **1981**, *24*, 2485.
(38) Wang, H. T.; Felps, W. S.; Findley, G. L.; Rau, A. R. P.; McGlynn, S. P. *J. Chem. Phys*. **1977**, *67*, 3940.
(39) Herzberg, G. *Atomic Spectra and Atomic Structure*; Dover: New York, 1944.
(40) Koeckhoven, S. M.; Buma, W. J.; de Lange, C. A. *J. Chem. Phys*. **1993**, *99*, 5061.
(41) McGlynn, S. P.; Wang, H.-t.; Findley, G. L.; Felps, W. S.; Rau, A. R. P. *Spectrosc. Lett*. **1979**, *12*, 631.
(42) Dagata, J. A.; Scott, M. A.; McGlynn, S. P. *J. Chem. Phys.* **1988**, *88*, 9.
(43) Baig, M. A.; Connerade, J. P.; Dagata, J.; McGlynn, S. P. *J. Phys. B: At. Mol. Phys*. **1981**, *14*, L25.
(44) Lu, K. T. *Phys. Rev. B* **1971**, *4*, 579.
(45) Dagata, J. A.; Felps, W. S.; McGlynn, S. P. *J. Chem. Phys*. **1986**, *85*, 2483.
(46) Van Vleck, J. H. *Phys. Rev*. **1932**, *40*, 544.